Engineering Structures 247 (2021) 113125

Contents lists available at ScienceDirect

Engineering Structures

journal homepage: www.elsevier.com/locate/engstruct

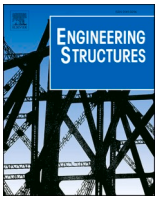

Mechanical performance of timber connections made of thick flexible polyurethane adhesives

Jaka Gašper Pečnik [a,b], Igor Gavrić [a,b], Václav Sebera [a], Meta Kržan [c], Arkadiusz Kwiecień [d], Bogusław Zając [d], Boris Azinović [c,*]

[a] InnoRenew CoE, Livade 6, 6310 Izola, Slovenia
[b] University of Primorska, Titov trg 4, 6000 Koper, Slovenia
[c] Slovenian National Building and Civil Engineering Institute, Dimičeva ulica 12, 1000 Ljubljana, Slovenia
[d] Cracow University of Technology, Warszawska 24, 31-155 Kraków, Poland

ARTICLE INFO

Keywords:
Flexible adhesive
Timber connection
Polyurethane
Double lap-shear
Cyclic loading
Energy dissipation

ABSTRACT

This study investigates timber connections with flexible polyurethane adhesives, which prove to have the potential for timber-adhesive composite structures without mechanical connections for seismic regions. Results of conducted cyclic double lap-shear adhesive timber joints tests were compared with available experimental results on timber connections with standard mechanical dowel-type fasteners and with results of numerical finite element analysis. The study found that the shear strength, elastic stiffness and strength degradation capacity of the flexible adhesive connections were significantly higher compared to mechanical fasteners commonly used in seismic-resistant timber connections. The latter, however, manifested larger ultimate displacements but also yielded at lower displacements.

1. Introduction

Mass timber, especially cross-laminated timber (CLT), is becoming an increasingly popular building material in Europe and across the world. The versatility of CLT has encouraged engineers to build from low to tall rise buildings. CLT panels perform in high stiffness, resistance to shear, tension and compression in-plane, and act in low ductility and dissipation of energy [1]. The connections between the CLT elements play a key role in ductility and energy dissipation of timber structures in addition to providing sufficient stiffness and strength between the structural elements and, thus, require special attention [2]. Therefore, the behaviour of CLT buildings during earthquakes depends mainly on the performance of connections between adjacent panels and other structural elements [3]. Several full-scale CLT building tests showed that damage and eventual failures during earthquakes are primarily localized in connections. When connections are too rigid, large accelerations can occur in the upper stories due to the lightweight nature of timber structures [4]. This may result in injuries to occupants and damage to property, which is not acceptable in terms of serviceability. Therefore, the structural system should be adapted by incorporating elements with sufficient strength and desired stiffness, which possibly reduces the structural damage through different energy dissipation mechanisms. This is typically achieved by applying mechanical dissipative connections that are installed in various parts of the structure, where deformations and, consequently, energy dissipation are desired. Furthermore, these elements are usually designed to have sufficient ductility to sustain extreme loads to prevent brittle failure of structural elements in case of extreme seismic events. They are usually not cost-effective or even feasible to design in order to sustain such high strength and displacement demands without significant damage. In addition to standard fastening solutions such as dowel-type fasteners (nails, screws, dowels) and metal connectors (hold-downs, angle brackets, nail plates), which cause plasticizing of timber under cyclic loads [5,6], several solutions for dissipative connections have already been suggested to improve the ductile response of CLT buildings [7–13]. These solutions have been mainly focused on mechanical connections with concentrated plasticity. In such systems, the dissipation is concentrated in a small area that must be very carefully designed to prevent damage to other parts of the structure. Moreover, plasticized connectors must be exchanged for new ones to continue the protection

* Corresponding author.
E-mail addresses: jaka.pecnik@innorenew.eu (J.G. Pečnik), igor.gavric@innorenew.eu (I. Gavrić), vaclav.sebera@innorenew.eu (V. Sebera), meta.krzan@zag.si (M. Kržan), akwiecie@pk.edu.pl (A. Kwiecień), bozajac@pk.edu.pl (B. Zając), boris.azinovic@zag.si (B. Azinović).

https://doi.org/10.1016/j.engstruct.2021.113125
Received 31 January 2021; Received in revised form 29 July 2021; Accepted 31 August 2021

of a structure.

On the other hand, recent studies of adhesive bonding show several advantages. Adhesive connections can exhibit uniform stress distribution along the connection and, therefore, can reduce localized high stresses [14,15]. Mechanical fasteners may, on the other hand, cause undesired damage in the wood fibrous structure, introducing local stress concentrations [5,6], and cause bridging water into the wood structure [16]. In addition, they contribute to weight, cost, presence of corrosive elements and require additional machining operations [17]. Furthermore, damages caused by mechanical fasteners during ductile behavior of connections result in irreversible deformations of the structure, which may result in demanding and expensive repair after the earthquake. Elastic joining of structural elements and use of highly deformable adhesives have been successfully used for flexible joints or fibre grids for seismic strengthening of reinforced concrete frames with brick masonry infills [18]. Such polyurethane-based flexible adhesives have been studied for increasing the ductility of existing structures by repairing composite-to-brick bond or concrete elements [19–21].

Studies related to timber have been looking at the use of flexible adhesives for improving bending resistance of beams [22,23], comparison of rigid and flexible adhesives to connections with screws [24] and tensile loading performance of bonded timber elements with brittle and ductile adhesives [25] as well as studying the behaviour of joints for prefabricated timber structures [26] and repair of historical timber structures [27]. Recent innovation showed applications of polyurethane butt-joint bonding for structural timber bonding [28]. Shear characteristics are usually decisive in the design of durable timber adhesive bonds [29,30]. For thin bondlines, the methods for shear testing are well-established and standardized [31], while on the contrary, flexible adhesives are not commonly addressed from a mechanical perspective. Thick flexible adhesive bonds exhibit higher deformations, have better load transfer, and absorb more energy over impact events than rigid thin bondlines. Additionally, their damping capacity is beneficial since it reduces the transfer of noise and undesirable vibrations between timber elements, while the more uniform distribution of shear stresses in the thick adhesive bondlines can also result in better fatigue resistance [32], resistance to seismic action [18] and improved damping properties [33]. Bondline thickness and overlap length are important characteristics for the mechanical performance of joints with flexible adhesives. As reported by Banea and Silva [34], increasing bondline thickness results in decreasing joint strength, while increasing overlap length improves rigidity of the joint. Scale effect was proven in the case of NSM (near surface mounted) composite strengthening application with PS adhesive loaded in shear, where small-scale specimen tests on flexible adhesives [35] manifested lower effectiveness than the same system applied in large-scale specimens [36].

Characteristics of flexible adhesives indicate opportunities for applications in timber constructions for either mechanical or physical improvements. Therefore, the objective of this paper is to identify the potential of thick flexible adhesive bondlines as a dissipative connection in timber structures in seismic-prone areas as a possible addition or alternative to common traditional timber connections. Possibilities of innovative timber connections with thick flexible polyurethane adhesives will be examined for application in seismic areas. These types of connections could serve as dissipative connections or high strength and high stiffness elastically deformable non-dissipative connections. One of the possible applications for such adhesives in CLT connections could be in vertical step joints between adjacent CLT wall panels, which behave with reduced stiffness but exhibit higher displacement capacity under cyclic loading compared to single layout monolithic CLT wall panels [37,38]. Large overlapping areas in step joints and dissipative capabilities make this type of connection a good candidate for improvements with flexible adhesives. Increasing the number of coupled panels into smaller segments would allow more panel rocking movement during seismic events. Additionally, the application of timber connections with thick flexible polyurethane adhesives could serve for flexible glued-in rod connections in timber structures and other types of structural connections such as steel-to-timber flexible connections and potentially even in structural glass-to-timber connections, where additional elastic flexibility with sufficient strength capacity would be desired. Further, secondary and non-load bearing elements in buildings that are sensitive to brittle failures during seismic events (such as large windows) could be additional field of application of these type of innovative connections in buildings. To verify such application, this paper fully describes the mechanical behaviour of thick flexible adhesive bondline exposed to monotonic and reversed cyclic loading.

The study highlights the following goals: (i) evaluation of mechanical characteristics of timber connections using three different flexible adhesives and two different bondline thicknesses obtained under monotonic and reverse cyclic loading; (ii) theoretical/analytical comparison of results to mechanical properties of standard dowel-type fasteners used in current CLT building applications; (iii) finite element model design for further investigation of bondline characteristics and its effect on the mechanical performance of flexible adhesive joints.

2. Materials and methods

2.1. Specimens and adhesives

Double lap-shear wood samples were made from Norway spruce (*Picea abies* L.). First, the wood was cut into elements with dimensions 30 × 35 × 200 mm (width × thickness × length) for middle parts and 20 × 35 × 200 mm for side parts of the specimen. Surfaces of adherends were coated with SIKA ZP Primer as recommended by the producer [39]. After 24 h of drying, the primer, double lap-shear forms with targeted thickness gaps between the adherends and 100 mm overlap length were assembled. Gaps and open spaces in the specimen geometry were closed using blocks of extruded polystyrene to prevent the adhesive from leaking. The middle timber part of the double lap-shear specimen was increased in width by adding two smaller timber blocks to each side to provide a greater clamping area for testing grips.

Three different types of two-component polyurethane-based adhesives, originated from SIKA Poland, were used in this study. To evaluate the mechanical characteristics of the adhesives, 6 specimens of each were tested in tension with a 5 mm/min loading rate (Fig. 1). To derive the material model for the finite element (FE) model of lap shear, arithmetic mean curves (thick lines in Fig. 1) were transferred into 7–12 stress–strain points. Adhesive PS has the highest modulus of elasticity but the lowest strength and elongation at break; PTS has a larger elongation at break than PS but the lowest modulus of elasticity; PST adhesive has the highest tensile strength and modulus of elasticity and elongation at break between PS and PTS (Fig. 1).

For the construction of specimens for double-lap shear testing of timber connections with the flexible adhesives, all adhesives' components were precisely weighed according to the producer's instructions on the component ratios and stirred together using a hand pistol and a mixing tool. The adhesive was poured into the double lap-shear timber-molds and dried for 24 h. No additional pressure was applied on the adherend. After the adhesive had hardened, the specimens were again planed to the final thickness of 30 mm and the excess adhesive on the top was removed to assure a plain surface. The specimens were stored in a climate chamber at (20 ± 2)°C and (65 ± 5) % relative humidity for at least one week before the first test started.

For each of the three selected adhesives (PS, PST, PTS), two different thicknesses (10 and 15 mm) were used, resulting in a total of 6 sample groups. A number of at least 4 repetitions for monotonic tests and cyclic tests for each type of adhesive and each bond-line thickness was chosen prior to the experimental campaign. For this, a limited number of specimens was produced in advance, and the tests were performed on all available specimens. In some cases, the specimen production was not successful due to out-of-factory conditions (non-uniform adhesive consistency, trapped air bubbles in specimens, etc.), and therefore, the

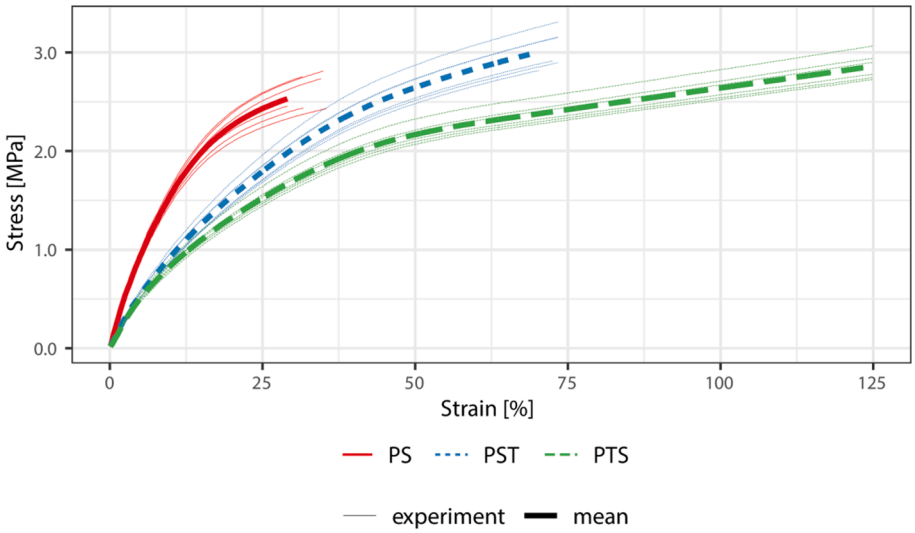

Fig. 1. Stress–strain relationship of the tested PS, PST and PTS adhesives (mean values in bold).

specimens were not suitable for tests. To provide additional valuable information, such as the influence of the number of specimens on the variance of the mechanical properties, all suitable specimens were tested, and all the obtained results are presented in the paper. Therefore, 4 monotonic tests and 4–8 cyclic tests were performed within each of the groups for a total of 55 double lap-shear tests (Table 1).

The specimen labelling is uniform throughout the paper, indicating each group by type of adhesive, thickness (10 or 15 mm) and type of tests ("M" for monotonic, "C" for cyclic).

2.2. Experimental test design

Both cyclic and monotonic tests were performed on a universal testing machine (UTM) Zwick Roell Z050. The specimens were clamped with hydraulic grips on the top part (central element) and the bottom part (two side elements), applying 7.5 MPa side pressure, to prevent specimens from slipping. The top part of the specimen was fixed, while displacement-controlled loading was induced to the lower part with a loading rate of 5 mm/min.

First, monotonic tests were conducted to further design cyclic protocol according to ISO 16670 standard [40], a reverse cyclic testing method for mechanically joint fasteners. Ultimate displacements from force-displacement (*F-u*) curves obtained from monotonic tests were used to determine cyclic steps. Ultimate displacement (vu-b) of the specimens, i.e., failure, was defined as the point where the force decreases to 80 % of the maximum force (F_{max}). For each specimen group, average vu-b displacements from monotonic tests were used to determine group loading protocols. The test started when the specimen was in the neutral unloaded position, following the positive (downward) and negative (upward) direction. Loading protocol was strain-controlled over external linear position transducer (LPT) Novotechnik connected to a digital amplifier that was connected to UTM. Specimen setup during the testing phase is shown in Fig. 3.

To fully characterize mechanical properties from cyclic test results, a procedure from EN 12512 standard [41] was combined with ISO 16670 [40]. Elastic and plastic stiffness values, forces and corresponding displacements at yield point, maximum strength point and failure point, and ductility values were for results of both monotonic and cyclic tests assessed following the EN 12512 procedure. For cyclic tests, equivalent viscous damping ratio and strength degradation were also calculated for each loading cycle (see Section 3). Additionally, average values of ultimate shear strain at the failure point (γ_u) were derived as a ratio between ultimate displacement (u_u) and adhesive thickness (t), maximum shear strength (f_{max}) as a ratio between maximum force and the total bond area (A), and shear modulus *(G) as* a ratio between shear stress at the yield point ($f_y = F_y / A$) and shear strain at the yield point ($\gamma_y = u_y / t$).

Table 1
Double lap-shear test schedule (M – monotonic, C – cyclic).

Name	Adhesive thickness [mm]	No. of tests(M/C)	
PS-10-M	PS-10-C	10	4/4
PST-10-M	PST-10-C		4/5
PTS-10-M	PTS-10-C		4/8
PS-15-M	PS-15-C	15	4/4
PST-15-M	PST-15-C		4/6
PTS-15-M	PTS-15-C		4/4

2.3. Numerical model

The physical tests – double lap-shear – carried out on the UTM was modelled using finite elements (FE) implemented in software Ansys 19.1 R1 (Ansys® Academic Research, Release 19.1) [42]. The specimen geometry, material composition and boundary conditions reflected the physical test on UTM, although the geometry was modelled as plane-stress with a defined thickness (Fig. 2).

Both wood material and adhesive were modelled using solid quadratic finite element PLANE183. Wood was modelled as linear elastic orthotropic material, adhesives were modelled as hyper-elastic material using two-parameter Yeoh model (YM2), see Table 2. Parameters of YM2 were obtained by curve-fitting the spline curves that interpolated data given from the experiments (Table 2), parameters d_1 and d_2 of YM2 were equal to zero for all adhesives. The curve fitting to YM2 was carried out in Ansys 19.1 [42].

The contact of wood with steel grips from the UTM was neglected as the boundary conditions were applied directly to the nodes of the wooden component. The connection between the adhesive and wood was defined as fully fixed, so no debonding was considered. The element size was set to 5 mm for wooden parts, but the adhesive element size reflected the thickness of the adhesive layer. The total number of elements/nodes was approximately 1100/3500 for a scenario with 10 mm thick adhesive. The geometrical model does contain right angles with infinitely small radii because stress and strain at corners was not analysed in our work. The FE model enabled us to perform a sensitivity study on the influence of adhesive thickness on resulting *F-u* response and stress distribution along horizontal and vertical paths cutting the specimen (see Fig. 2).

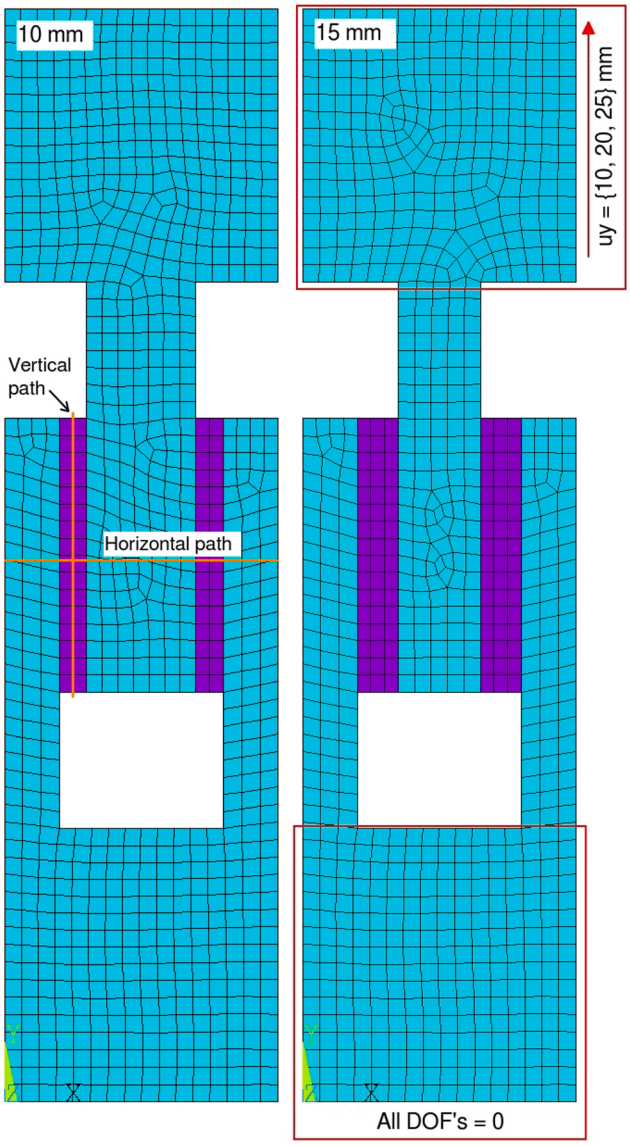

Fig. 2. Finite element mesh for adhesive bonds of 10 mm and 15 mm thickness, including defined paths and boundary conditions of nodes in red rectangles. Colours represent different material (wood vs. adhesive).

3. Results and discussion

3.1. Failure mechanisms

Initial deformations were, as expected, a result of elastic shear deformations of the adhesive due to considerably higher flexibility of the adhesive in comparison with wood. In general, four different failure scenarios were observed, as presented in Fig. 3. In most cases, failure occurred in the area between adherend and adhesive as a consequence of debonding at the interface between wood and adhesive.

In both testing regimes, the adhesive peeled from the adherend either on the edge of the inner or the edge of the outer side of the adhesive bond. It was also often observed that the peeling started on the top of adherend in either the inner or outer side and propagated to a certain length and then further propagated on the opposite side until significant stress reduction occurred (Fig. 3a, 3b). Particularly under the cyclic test, the peeling was also present on the bottom side of the adherend under compression loading of the specimen (positive direction). Under cyclic loading, the peeling in the middle adherend propagated with every cycle and with every increase in displacement step. Thicker (15 mm) PTS and PST bondlines often also exhibited failure in the adhesive (Fig. 3c). Rarely, brittle failure occurred in wood in the central or side component due to exceeded strengths combined by tension perpendicular to grain and shear parallel to the grain. This was especially caused by eccentricity in loading in the latter phase of the test, where unequally peeled adhesive on either side of the sample caused slight rotation of the timber elements (Fig. 3d). In such cases, specimens were eliminated from further analyses.

Table 2
Material properties used in FE analyses.

Material	Orthotropic elastic		
Spruce*	$E_L = 14850$ MPa, $E_R = 352$ MPa, $E_T = 289$ MPa, $G_{LR} = 573$ MPa, $G_{RT} = 53$ MPa, $G_{LT} = 474$ MPa, $\nu_{LR} = 0.023$, $\nu_{RT} = 0.557$, $\nu_{LT} = 0.014$ [-]		
	Isotropic hyperelastic	Yeoh model parameters	
	Strain/Stress [-/MPa]	C10 [MPa]	C20 [MPa]
PS	0/0.022, 0.05/0. 938, 0.1/1.555, 0.15/1.984, 0.2/2.257. 0.25/2.4316. 0.3/2.531	−2.977	−2.812
PST	0/0.0173, 0.1/0.933, 0.2/1.541, 0.3/2.025, 0.4/2.392, 0.5/2.645, 0.6/2.838, 0.7/3.001	1.578	−0.241
PTS	0/0.0173, 0.1/0.840, 0.2/1.321, 0.3/1.701, 0.4/1.983, 0.5/2.168, 0.6/2.286, 0.7/2.377, 0.8/2.466, 0.9/2.554, 1/2.641, 1.1/2.727, 1.2/2.816, 1.26/2.869	1.167	−0.092

E, G, and ν denote normal and shear moduli and Poisson's ratio, respectively; Indices L, R, T stand for anatomical directions of wood – longitudinal, radial and tangential, respectively. * Data taken from [43].

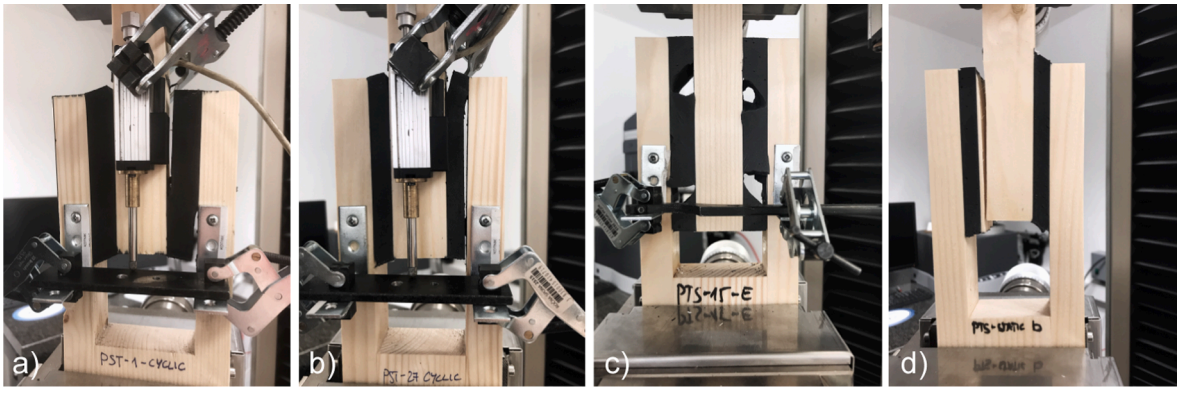

Fig. 3. Four typical types of failure: peeling on the side of the middle adherend (a), peeling on the side of a side adherend (b), dissipative adhesive failure (c), brittle failure in the adherend (d).

3.2. Monotonic tests

Force-displacement (*F-u*) diagrams for three types of adhesive and both thicknesses are depicted in Fig. 4 with some notable differences visible for both thicknesses and adhesives. For all adhesives, a higher maximum force (F_{max}) was reached for thinner bondlines. Displacement at F_{max} (D_{max}) grows in order of adhesives PS, PST, and PTS, respectively and also implies their hyper-elastic behaviour. Dashed lines in Fig. 4 indicate results of FE analyses based on material data (Fig. 1). The relative difference (RD) of stiffness (K_{el}) between FE models and experiments (Table 3) is given by RD = (X_{FEM}/X_{EXP} -1) * 100. The RD for PS, PST and PTS adhesives for both thicknesses (10 and 15 mm) is following: 54 and 39 %; 24 and 7.3 %, 14 and 38 %. It is clear that all FE models are overestimating K_{el} compared to experiments, which is due to a fact the experiments always contain certain imperfections in material and boundary conditions contrary to flawless FE models. Numerical prediction of bondline strength using F_{max} and D_{max} is complicated since FE models do not have adhesion strength between wood and adhesive defined, which showed to be a key factor reducing bond strength in the experiments. Besides that, FE models do not fail at higher thicknesses either due to tremendous strain at failure of the adhesives, so their comparison with experiments is very limited and omitted here. However, the simulated *F-u* curves exhibit clearly that predicted F_{max} are or would be higher than experimental ones. To overcome the limitation of strength predictions of such FE models, one has to combine fracture mechanics models defined on an interface of wood and adhesive, together with presented hyperelastic material models. Nonetheless, even though this work showed importance in definition of fracture models to predict strength of such bonds, it was not aim of this work and, therefore, it is kept as a task for further research.

In Table 3, average values of evaluated mechanical properties from monotonic tests for each specimen group are presented, together with standard deviation values and coefficient of variance.

The highest elastic stiffness and shear modulus were achieved in PS adhesives, followed by PST adhesives, while the lowest stiffness was for PTS adhesive. With increased bondline thickness, the elastic and plastic stiffness were reduced by 25 %, on average, for all three adhesives. Among 15 mm thick bondlines, PS showed the highest stiffness. PTS-15 showed the lowest stiffness, with an average of 45 % lower values compared to the PS-15 group, while PST-15 resulted in a 30 % lower elastic stiffness value compared to PS-15. Average strength capacities were found to be higher for 10 mm thick adhesives descending from PST-10, PTS-10 and PS-10 with 1.74 MPa, 1.71 MPa and 1.48 MPa, respectively. The difference in average strength capacity between PS, PST and PTS adhesives with 15 mm in thickness compared to 10 mm showed values decreased by 19 %, 32 % and 19 %, respectively. The achieved strength capacity values were significantly lower in all cases compared to the measured tensile strength values (Fig. 1). This can be attributed to the fact that the full-strength capacity of the adhesive could not be achieved due to the weaker strength capacity of the bond between the adherent and adhesive, as previously reported in Section 3.1 and shown in Fig. 3. To achieve higher strength capacities of such lap-shear connections, the bond strength capacity between wood and adhesive should be enhanced by roughening the wood surface or optimizing the primer to achieve higher adhesion capacity between wood and adhesive. In terms of deformability, PTS-15 adhesive exhibited significantly better performance, namely 1.8 times and 2.3 times higher displacement capacity and ultimate shear strain compared to PST-15 and PS-15 adhesives, respectively. The effect of adhesive thickness was not as pronounced, namely the differences between average values of 10 mm and 15 mm thick adhesives varied between 8 and 14 %, while achieved ultimate shear strain values were significantly higher in 10 mm thick adhesives compared to 15 mm (31–71% difference). Further, PTS adhesive showed the highest ductility (ratio between ultimate displacement and yield displacement) among all adhesives and both thicknesses. PTS-15 exhibited 21 % and 7 % higher ductility than PST-15 and PS-15, respectively. In the case of thinner bondlines, the PTS-10 group showed only 8 % and 2 % higher ductility compared to PST and PS adhesive, respectively. Similarly, as in the case of displacement capacity, ductility values were not affected by increased bondline thickness, namely the ductility values increase or decrease was 10 % or less in all three adhesives.

3.3. Cyclic tests

Overall behaviour, in terms of strength and deformation capacity, and failure mechanisms in cyclic tests correlated with the prior observations from monotonic tests. Typical hysteresis loops for each group in Fig. 5 display the effects of thickness and type of adhesive by different shape of the hysteresis loops, number of achieved steps and loading cycles. The shapes of the hysteresis loops are not like typical mechanical timber connection or timber wall elements using mechanical fasteners [3,37,38], namely flexible adhesive hysteresis loops display a considerably higher proportion of elastic deformability; while on the other hand, they usually display lower plastic deformation capacity. In addition, recovery stiffness in 2nd and 3rd cycles at the same amplitude displacement is more linear than in the case of mechanical connections, as there is no effect of metal fasteners embedment into the wood. Moreover, the level of the stiffness reduction after the 1st cycle is generally lower in the case of flexible adhesive connections as there is no

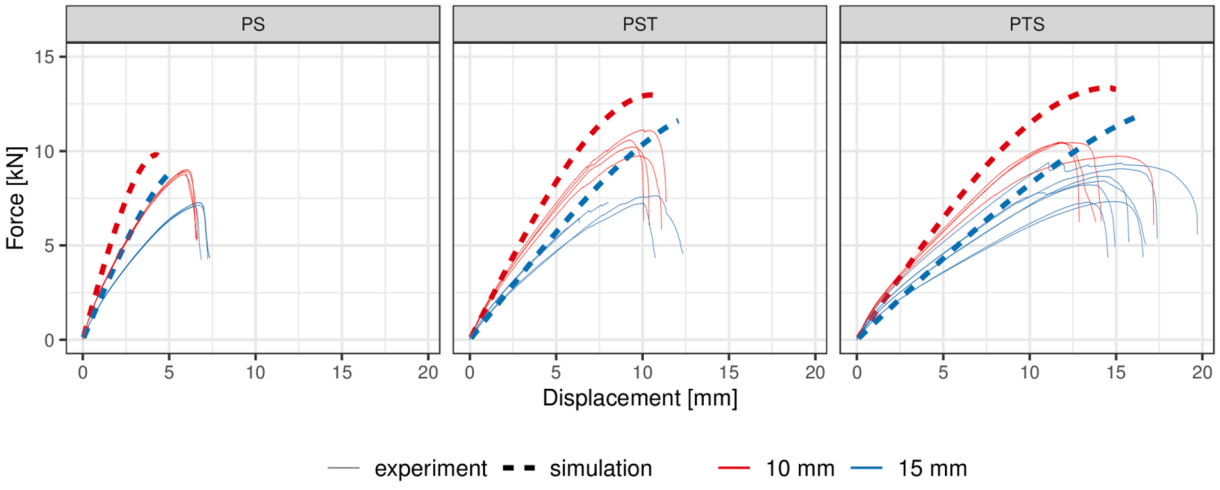

Fig. 4. Force-displacement diagrams of monotonic tests for different adhesives and thicknesses (10 mm thickness in red, 15 mm thickness in blue).

Table 3
Average values of mechanical properties from monotonic test results: elastic and plastic stiffness (k_{el}, k_{pl}), shear modulus (G), force and displacement at the yielding point, (F_y, u_y), maximum load (F_{max}), displacement at maximum force (u_{Fmax}), maximum shear strength (f_{max}), ultimate load ($F_{u\text{-}80\%}$), ultimate displacement (u_u), ultimate shear strain (γ_u), and ductility (D).

Adhesive	k_{el} [kN/mm]	G [MPa]	k_{pl} [kN/mm]	F_y [kN]	u_y [mm]	F_{max} [kN]	u_{Fmax} [mm]	f_{max} [MPa]	$F_{u\text{-}80\ \%}$ [kN]	u_u [mm]	g_u	[-]	D [-]
PS-10-M	avg	2.13	3.68	0.35	8.13	3.68	8.90	5.93	1.48	7.12	6.45	0.65	1.75
	stdev	0.03	–	0.00	0.11	0.07	0.11	0.11	0.02	0.09	0.06	–	0.03
	cov [%]	1.23	–	1.23	1.33	1.96	1.26	1.87	1.26	1.26	0.98	–	1.59
PS-15-M	avg	1.55	4.01	0.26	6.53	4.07	7.18	6.64	1.20	5.74	7.03	0.47	1.73
	stdev	0.01	–	0.00	0.09	0.04	0.10	0.10	0.02	0.08	0.20	–	0.04
	cov [%]	0.58	–	0.58	1.39	0.94	1.43	1.55	1.43	1.43	2.90	–	2.51
PST-10-M	avg	1.44	2.49	0.24	9.68	6.49	10.41	9.63	1.74	8.33	10.64	1.06	1.64
	stdev	0.05	–	0.01	0.57	0.20	0.59	0.36	0.10	0.47	0.57	–	0.10
	cov [%]	3.51	–	3.51	5.90	3.04	5.64	3.78	5.64	5.64	5.36	–	6.23
PST-15-M	avg	1.09	2.75	0.18	6.69	6.08	7.15	8.77	1.19	6.33	9.16	0.61	1.49
	stdev	0.13	–	0.02	0.41	1.03	0.50	2.00	0.08	0.63	2.45	–	0.16
	cov [%]	12.15		12.15	6.06	16.89	7.04	22.76	7.04	9.95	26.79	–	11.09
PTS-10-M	avg	1.13	1.98	0.19	9.47	7.98	10.27	12.66	1.71	8.22	14.26	1.43	1.79
	stdev	0.04	–	0.01	0.57	0.36	0.36	1.66	0.06	0.29	1.99	–	0.32
	cov [%]	3.32	–	3.32	6.03	4.45	3.51	13.09	3.51	3.51	13.93	–	17.91
PTS-15-M	avg	0.85	2.19	0.14	7.66	8.75	8.34	13.76	1.39	6.67	16.31	1.09	1.88
	stdev	0.13	–	0.02	0.75	0.75	0.81	1.34	0.13	0.64	1.69	–	0.32
	cov [%]	15.66	–	15.66	9.85	8.54	9.67	9.76	9.67	9.67	10.37	–	17.02

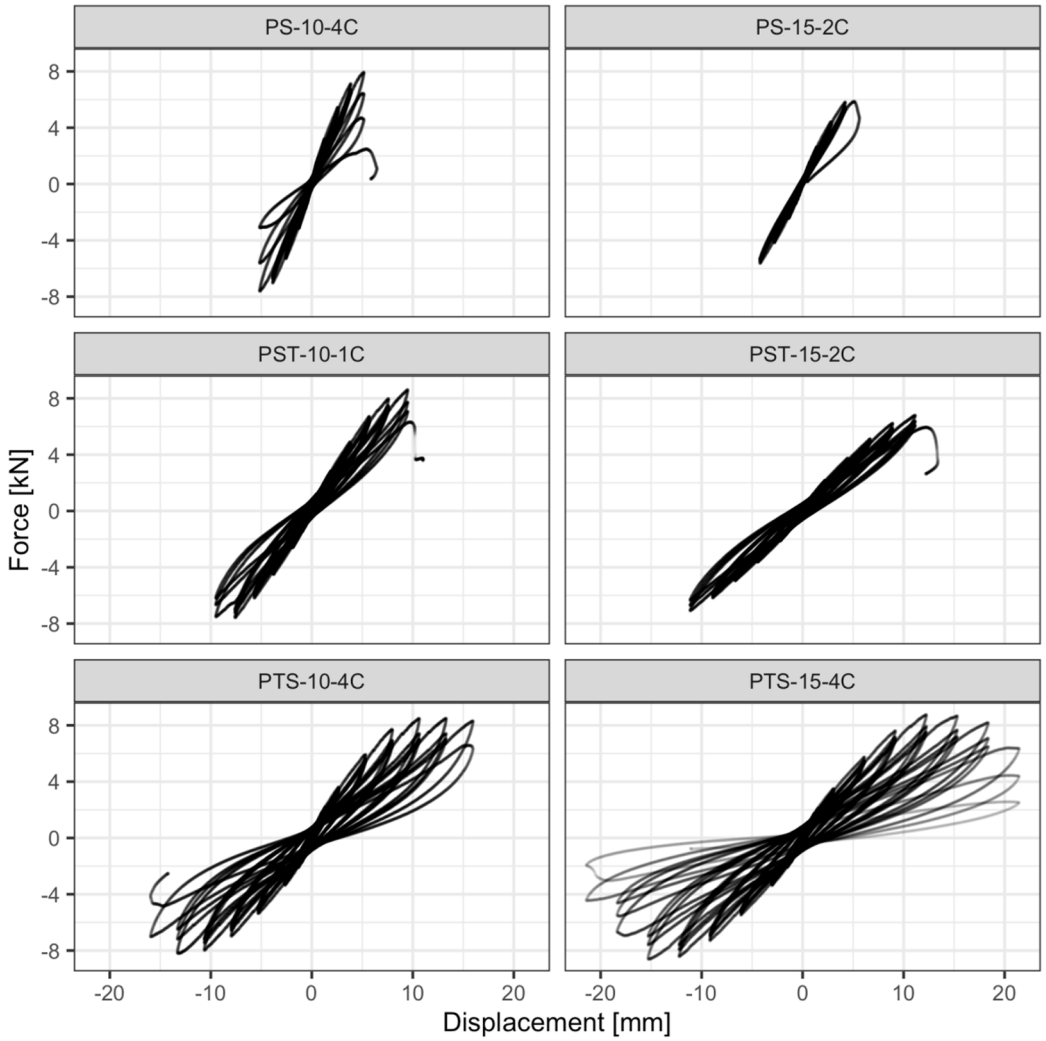

Fig. 5. Examples of typical hysteresis curves for each test group from cyclic testing.

formed gap between the fastener and wood, as is the case in mechanical connections. In the case of flexible adhesive connection, the connection between the wood and adhesives remains intact in the linear part of the response; while in the non-linear part, the stiffness reduction is due to partial peeling of the adhesive, which causes gradual progressive stiffness reduction. In addition, the hysteresis shapes differ in the unloading part of the cycles, where the force drop in mechanical connections is usually rapid, and the force drop in the case of adhesive connections is more gradual. Consequently, this results in a smaller hysteresis loop area, which indicates lower energy dissipation capacity. Further comparison among flexible adhesive connections' cyclic behaviour properties from this study is directly compared with corresponding mechanical connection's properties in Section 3.4. The least flexible PS adhesive shows better performance with a thinner adhesive layer, while in the case of two other types of adhesives, the thicker bondline outperforms the thinner one. Fewer loading steps were also reached for PS than PST or PTS in the case of the thicker bondline.

Fig. 6 displays backbone curves for all cyclic tests performed for six different test groups. A comparison was done for different types of adhesives and different thicknesses among the same type of adhesive. Bold lines present 10 mm adhesive thickness, while dashed lines present 15 mm adhesive thickness. Typically, slightly higher ultimate displacements are met for thicker bondline in PS and PST cases, while in the case of PTS, more loading steps and, consequently, significantly larger ultimate displacements are reached. Inclination of the curve identifies decreasing stiffness among adhesives from less to more flexible.

In Table 4, strength and deformability properties evaluated from backbone envelope curves (Fig. 6) are presented by considering average values from the positive and negative part of loading in absolute values following the same assessment procedure as presented in Section 3.2.

Higher elastic and plastic stiffness were observed in tests with thinner bondlines among the tests with the same type of adhesive. For instance, the average k_{el} for PS, PST and PTS was 27 %, 29 % and 16 % lower in tests with 15 mm thick bondline. Percentwise, a similar reduction was observed for PS and PTS in the monotonic test, while a lower reduction was obtained in the case of the cyclic PTS group. Similar to in the monotonic test, again PS adhesive showed the highest elastic stiffness and PTS adhesive the lowest. In this case, the PTS-15 group showed, on average, 41 % lower stiffness in comparison to the PS-15 group. This result is close to the result of the monotonic test (45 % reduction), while greater stiffness reduction was also noticed for the PST-15 group with a 41 % reduction. On the other hand, comparison between monotonic and cyclic tests has shown that in the case of cyclic test, values for elastic stiffness were higher for all cases except for the PST-15 group that showed comparable value.

While PS adhesive displayed higher initial stiffness, its deformation capacity was much more limited compared to PST and PTS adhesives, while it also displayed slightly lower strength capacity compared to the other two adhesives. PTS adhesive performed with the highest deformation capacity, while also being the most flexible (the lowest elastic stiffness values). The strength capacity of PTS adhesive was comparable with PST adhesive.

In terms of ductility, the highest values were observed for PTS adhesive. The highest average value, of 2.37 for PTS-10, showed 44 % and 31 % higher ductility (D) against PST-10 and PS-10, respectively. PTS-15 group showed 4 % lower D against PTS-10, which overall resulted, on average, to 49 % and 47 % higher D against PST-15 and PS-15 group, respectively. Similar to stiffness, the ductility was lower for thicker bondline with a 4 %, 7 % and 14 % decrease in the group for PTS, PST and PS, respectively. The most significant increase between monotonic and cyclic test was found for PTS adhesive with almost 1.2 and 1.3 higher D for 15 and 10 mm thick bondline.

Average strength degradation between the 1st and the 3rd loading cycle (ΔF_{1-3}) for each group separated by adhesive thickness is presented in Fig. 7. Strength degradation values are a measure of percentage difference in force drop at a certain displacement step between the 1st and the 3rd loading cycle. This mechanical property indicates the connection's behaviour under low cycle fatigue events such as earthquakes. Average strength degradation was derived from the total number of specimens per cyclic group test. Overall, five amplitude displacement steps were considered to show adequate information, except in the case of PS adhesive where only three steps were used due to early failure of the specimen. Comparing 10 mm and 15 mm thick bondline, lower strength degradation was obtained for thicker 15 mm adhesives bondline specimen in all three types of adhesives. The final displacement step shows the highest increase in strength degradation due to reaching the failure of the specimens. The average strength degradation at the failure point in the case of PS adhesives was less than 10 % in both cases (10 mm and 15 mm); while in cases of PST and PTS adhesives, these values were less than 20 % in all cases. According to the current version of Eurocode 8 [44], the dissipative connections shall be able to deform plastically for at least three fully reversed cycles without having more than a 20 % reduction of their resistance. This means that the analysed flexible adhesive connections satisfied this condition in all cases, yet none of the cases reaches a sufficient static ductility ratio of 4 to comply with ductility class DCM (medium capacity to dissipate energy). Therefore, in this current state, these connections are appropriate for use only in the DCL class (low capacity to dissipate energy) according to Eurocode 8 [44].

The equivalent viscous damping ratio (ν_{eq}) was calculated for the 1st

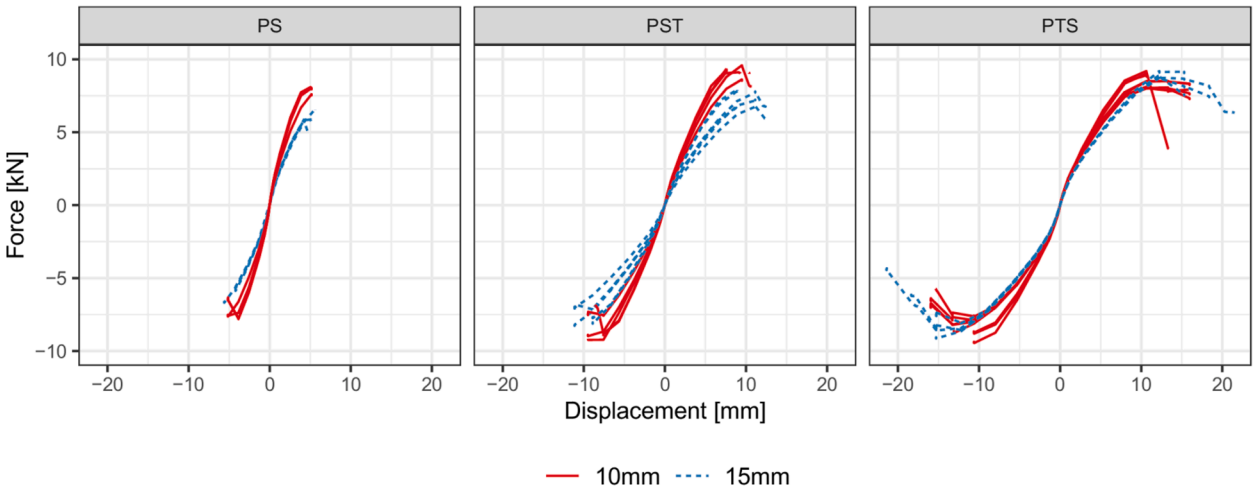

Fig. 6. Backbone curves obtained from cyclic testing of specimens with all three adhesives and both thicknesses.

Table 4
Average values of mechanical properties from cyclic test results: elastic and plastic stiffness (k_{el}, k_{pl}), shear modulus (G), force and displacement at the yielding point, (F_y, u_y), maximum load (F_{max}), displacement at maximum force (u_{Fmax}), maximum shear strength (f_{max}), ultimate load ($F_{u\text{-}80\%}$), ultimate displacement (u_u), ultimate shear strain (γ_u), and ductility (D).

Adhesive	k_{el} [kN/mm]	G [MPa]	k_{pl} [kN/mm]	F_y [kN]	u_y [mm]	F_{max} [kN]	u_{Fmax} [mm]	f_{max} [MPa]	$F_{u\text{-}80\ \%}$ [kN]	u_u [mm]	g_u	[-]	D [-]
PS-10-C	avg	2.37	4.07	0.40	7.01	2.87	7.78	4.97	1.30	7.35	5.16	0.52	1.81
	stdev	0.22	–	0.04	0.16	0.23	0.13	0.35	0.02	0.35	0.02	–	0.14
	cov [%]	9.34	–	9.34	2.23	8.04	1.70	7.07	1.70	4.82	0.44	–	7.57
PS-15-C	avg	1.74	4.46	0.29	5.60	3.14	6.01	4.67	1.00	5.86	4.87	0.32	1.55
	stdev	0.07	–	0.01	0.32	0.31	0.41	0.65	0.07	0.50	0.51	–	0.03
	cov [%]	3.94	–	3.94	5.76	9.77	6.89	14.01	6.89	8.49	10.41	–	1.68
PST-10-C	avg	1.47	2.51	0.24	8.36	5.55	9.04	8.53	1.51	8.51	9.18	0.92	1.65
	stdev	0.15	–	0.03	0.56	0.47	0.60	0.94	0.10	0.54	1.02	–	0.10
	cov [%]	10.38	–	10.38	6.70	8.53	6.62	11.03	6.62	6.31	11.07	–	5.76
PST-15-C	avg	1.03	2.61	0.17	6.85	6.55	7.37	9.63	1.23	7.13	10.04	0.67	1.53
	stdev	0.14	–	0.02	0.64	0.85	0.70	1.37	0.12	0.70	1.74	–	0.09
	cov [%]	13.28	–	13.28	9.34	13.01	9.55	14.19	9.55	9.77	17.25	–	6.13
PTS-10-C	avg	1.22	2.13	0.20	7.47	5.85	8.50	11.59	1.42	7.86	13.76	1.38	2.37
	stdev	0.07	–	0.01	0.50	0.19	0.48	1.18	0.08	0.80	2.51	–	0.47
	cov [%]	5.69	–	5.69	6.68	3.19	5.70	10.19	5.70	10.18	18.27	–	19.83
PTS-15-C	avg	1.02	2.66	0.17	7.84	7.36	8.75	12.98	1.46	7.65	16.75	1.12	2.28
	stdev	0.01	–	0.00	0.24	0.31	0.29	0.90	0.05	0.96	1.75	–	0.27
	cov [%]	1.39	–	1.39	3.06	4.15	3.32	6.92	3.32	12.58	10.44	–	11.79

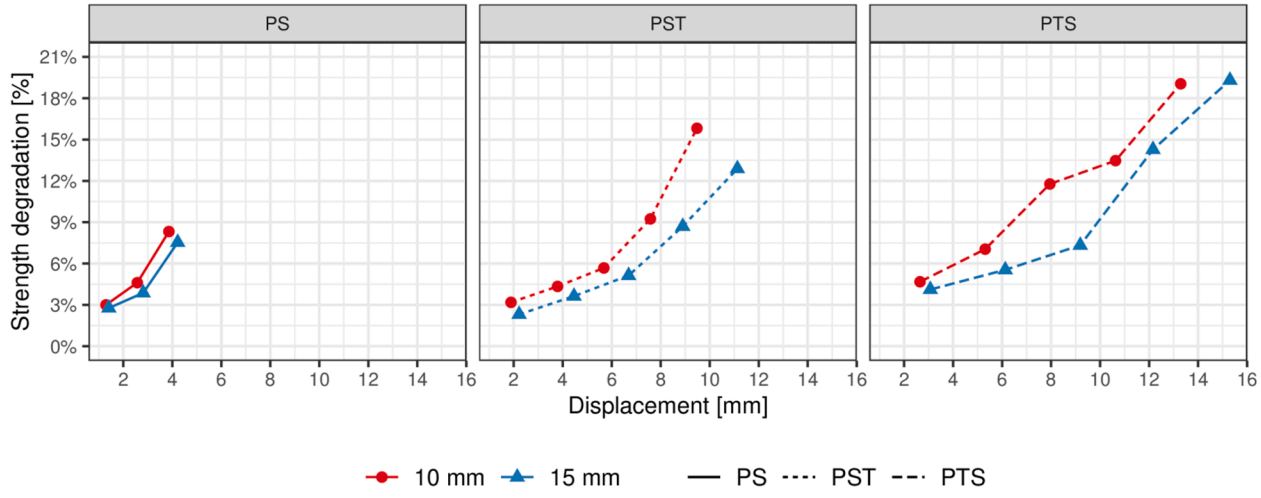

Fig. 7. Average strength degradation for 3rd cycles of loading compared to 1st cycles in % for each amplitude displacement step for each group.

and 3rd cycles for all displacement steps, and it is summarized in Fig. 8a for the 1st cycles and Fig. 8b for the 3rd loading cycles. It is a non-dimensional parameter to represent the hysteresis energy dissipation capacity of a connection, expressed as a ratio between the dissipated energy in one-half cycle (the area of hysteresis) and approximation of exhibited potential energy multiplied by 2π [41]. The 3rd cycles ν_{eq} ratio represents the connection's behaviour in subsequent low cycle loads caused during a seismic event, while the 1st cycles represent the connection's response in the peak loads caused by a seismic event. Among the three different tested adhesives, PTS adhesive performed with the highest energy dissipation capacity, resulting in 3rd cycle ν_{eq} equal to 5.5–7.1 %, while these ranges were 3.9–5.5 % for PST adhesive and 2.0–2.9 % for PS adhesive. This finding is in correlation with connections' deformation capacity in the plastic region (expressed through ductility in Table 4), in which most of the hysteretic energy is dissipated.

3.4. Comparison with mechanical connections

A comparison between the most commonly used mechanical types of connection between parallel wall panels in CLT structures (so-called half-lap or step joint) and flexible polyurethane adhesive shear connections, investigated in this study, is presented in this section. The mechanical properties are compared with the values reported in a study by Gavric et al. [45] on cyclic behaviour of typical screwed connections for cross-laminated timber structures. The type of CLT connection chosen for the comparison is the so-called half-lap connection with self-tapping screws HBS Φ8x80 mm between parallel wall panels, which is considered as a dissipative connection between CLT wall panels, where in addition to strength and stiffness capacity to transfer seismic loads, also sufficient deformation capacity shall be provided due to rocking kinematic mechanism of CLT wall panels during seismic events [38]. Average experimental values of mechanical properties of half-lap connection in Gavric et al. [45] are evaluated according to EN12512 procedure, the same as in the study on flexible adhesive connections presented in this paper.

A direct comparison of mechanical properties is performed on a hypothetical L = 100 cm long connection with B = 5 cm overlap between two CLT wall elements, which is a generally used width for half-lap joints in CLT structures. Force related mechanical properties from the cyclic tests on double lap-shear adhesive connections presented in this study (see Table 5) are increased proportionally to the hypothetical connection's adhesive surface, while displacements remain at the same levels. Mechanical properties of half-lap screwed connection [45] are presented for a single screw and for a series of equally spaced screws

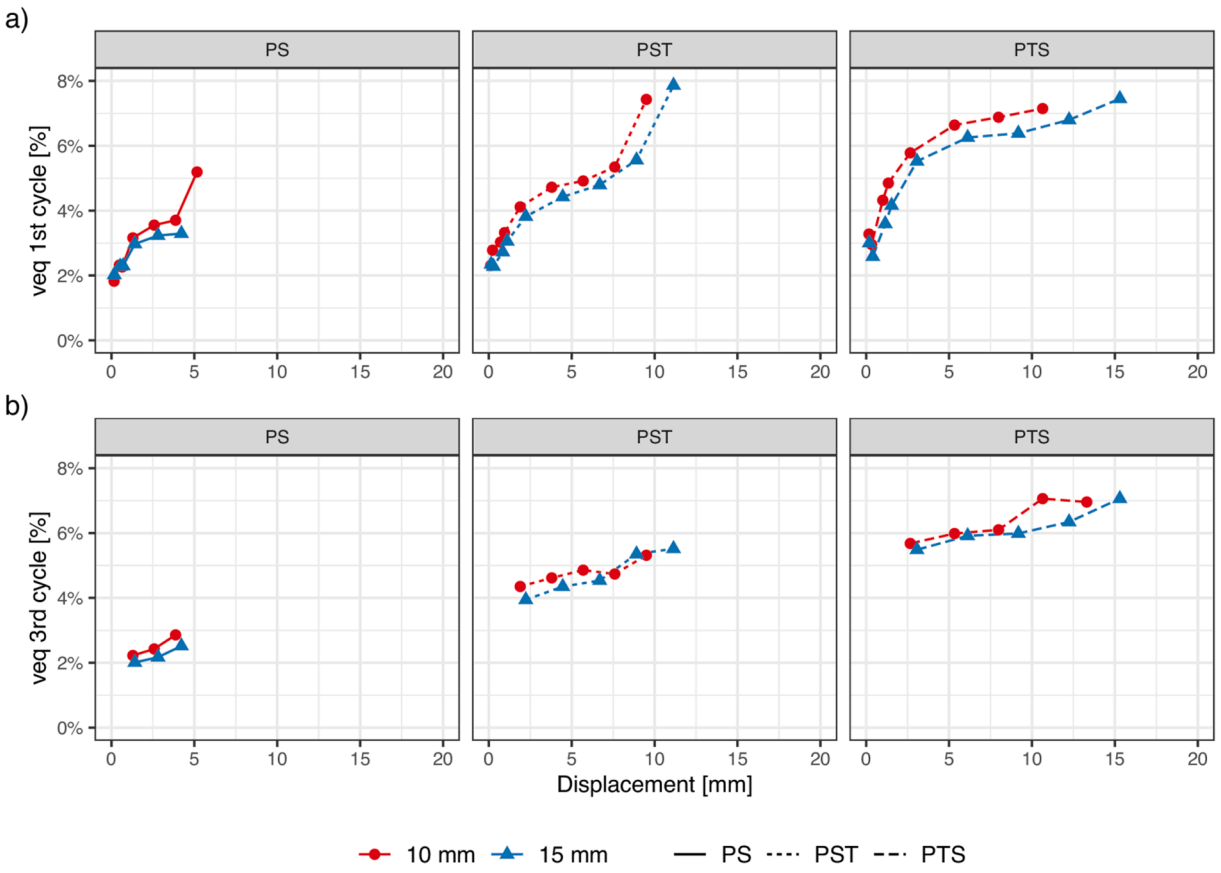

Fig. 8. Equivalent viscous damping ratio for a) 1st and b) 3rd loading cycles by type of adhesive and bondline thickness.

Table 5
Comparison of cyclic behaviour for mechanical properties of flexible adhesive connections and screwed half-lap CLT mechanical connections [45]: elastic and plastic stiffness (k_{el}, k_{pl}), force and displacement at the yielding point, (F_y, u_y), maximum load (F_{max}), displacement at maximum force (u_{Fmax}), ultimate load ($F_{u\text{-}80\%}$), ultimate displacement (u_u), and ductility (D).

Connection type	k_{el} [kN/mm]	k_{pl} [kN/mm]	F_y [kN]	u_y [mm]	F_{max} [kN]	u_{Fmax} [mm]	$F_{u\text{-}80\ \%}$ [kN]	u_u [mm]	D [-]
PS-10-C*	19.79	3.30	58.43	2.87	64.86	4.97	61.23	5.16	1.81
PS-15-C*	14.53	2.43	46.63	3.14	50.11	4.67	48.80	4.87	1.55
PST-10-C*	12.24	2.04	69.69	5.55	75.31	8.53	70.94	9.18	1.65
PST-15-C*	8.57	1.43	57.05	6.55	61.40	9.63	59.40	10.04	1.53
PTS-10-C*	10.17	1.69	62.23	5.85	70.85	11.59	65.52	13.76	2.37
PTS-15-C*	8.49	1.42	65.31	7.36	72.89	12.98	63.73	16.75	2.28
HBS Φ8 × 80 (1 screw)**	1.24	0.11	3.23	2.55	5.25	23.50	4.20	31.55	12.81
HBS Φ8 × 80 (e = 10 cm)	12.40	1.10	32.30	2.55	52.50	23.50	42.00	31.55	12.81
HBS Φ8 × 80 (e = 20 cm)	6.20	0.55	16.15	2.55	26.25	23.50	21.00	31.55	12.81
HBS Φ8 × 80 (e = 30 cm)	4.13	0.37	10.77	2.55	17.50	23.50	14.00	31.55	12.81

* calculated values for the connection length L = 100 cm and connection width B = 5 cm.
** average experimental test values reported in [45].

(spacing e = 10–30 cm) along the length of the connection, which is the most commonly used screw spacing range in CLT-to-CLT panel connections, where 30 cm spacing represents the most common structural spacing [46,47], while smaller spacings represent cases with higher structural demands.

In terms of elastic stiffness properties, all types of flexible adhesive connections exhibit significantly higher values compared to 30 cm spaced screwed connection. For example, PS adhesive connection results in 4.8 times and 3.5 times higher k_{el} for 10 mm and 15 mm adhesive thickness, respectively; while in the case of PST and PTS adhesives, these values range between 2.0 and 3.0 times the mechanical connection's k_{el}. To achieve the same k_{el} value as the most flexible adhesive connection PST-15, the screws would need to be spaced at 14.6 cm.

Comparison of strength properties shows that the selected adhesive connections have significantly higher strength capacity than all three screw spacing scenarios. Strengths of adhesive connections are 2.9–4.3 times higher than the strength of half-lap screwed connection with screw spacing of 30 cm. Therefore, to achieve the same level of strength capacity, the screw spacing would need to be in the range of 7.0–10.5 cm.

On the other hand, a screwed connection performs significantly better in terms of deformation capacity and ductility. Namely, the ultimate displacement capacity of the screwed connection is 6.1–6.5 times higher than in the case of PS adhesive connections, 3.1–3.4 times higher than in the case of PST and 1.9–2.3 times higher than the PTS. In all cases, the mechanical connection enters the plastic range (reaches the yielding point) at lower displacements than the adhesive connections. Consequently, the ductility values of the mechanical connection are 5.4–8.4 times higher than the ductility of analysed adhesive

connections.

Strength degradation as a result of low cycle fatigue is more pronounced in mechanical connection, reaching almost 30 % at the maximum strength point, while these levels in adhesive connections are less than 10 % for PS and less than 20 % for PST and PTS adhesives, as reported in Section 3.3.

Equivalent viscous damping ratio in the case of a screwed connection is averaging around 14.5 % in 1st cycles and 9.1 % in 3rd cycles at the maximum strength level [45], while these values are less than 10 % in 1st cycles and 2.9 %, 5.5 % and 7.1 % in 3rd cycles for PS, PST and PTS, respectively (see Fig. 8). Total dissipated energy in mechanical connection is additionally higher because it can withstand significantly higher ultimate displacements (Table 4 and Table 5).

3.5. Numerical sensitivity study

Numerical analysis aimed to investigate the influence of adhesive thickness on force–displacement (*F-u*) elastic response and stress in the adhesive. The *F-u* responses were used to calculate the relative change of elastic stiffness (k_{el}) with respect to the scenario with adhesive thickness of 1 mm (as shown for PS adhesive in Fig. 9c). It shows that stiffness decreases parabolically for all adhesives in a similar manner, but for PST and PTS adhesives it is more abrupt. Thicker bonds provide higher compliance and allow greater displacement before reaching strength level, which was confirmed also by the experiments (Fig. 4). This character may be used to an advantage in applications that need a relatively strong, but more flexible, adhesive bond. On average, k_{el} decreased by about 92–94 % when adhesive thickness changed from 1 mm to 20 mm. The relative change of F_{max} was not analyzed because F_{max} was not reached for thicker bondlines within the range of experimental displacements, which comes from the hyperelastic character of adhesives (Fig. 1). As discussed before, experiments showed that for all adhesives the failure of the specimen occurred at the interface with wood and not in the adhesive itself. Therefore, the limitation of FE models that generally provided higher values of *F-u* response has to be acknowledged when compared to experiments and that it did not cover debonding phenomena. This also means that the practical limitation of thick bonds lies in debonding, i.e., in the capabilities of primer to assure adhesion. To precisely predict the F_{max} with help of the FE model, it would be necessary to include fracture phenomenon at the interface. However, to describe the fracture behaviour of such bonds was not the aim of this research but may be a meaningful research aim for the future.

The distribution of stress on the specimen surface for 10 mm and 15 mm thick samples is shown in Fig. 9a. It can be seen that shear stresses are distributed symmetrically in the specimens, and that the highest strain occurs in adhesive bond (not shown). The stress was then analysed on two paths (black dashed lines in Fig. 9a): path cutting specimen in the middle of specimen height (horizontal line – H, Fig. 9d) and path going in the middle of adhesive vertically along the bondline (vertical line – V, Fig. 9b). The shear stress at the XY plane mapped onto these paths was created within the elastic deformation for all thicknesses at a displacement of 0.25 mm just for mutual comparison. Both paths show that increasing thickness of the adhesive substantially reduces maximal shear stress in adhesive, from ~ 3.5 MPa at 1 mm to ~ 0.13 MPa at 20 mm, which is ~ 29-fold reduction. Further, the horizontal path shows the highest shear stress occurs in the middle of the adhesive layer; the

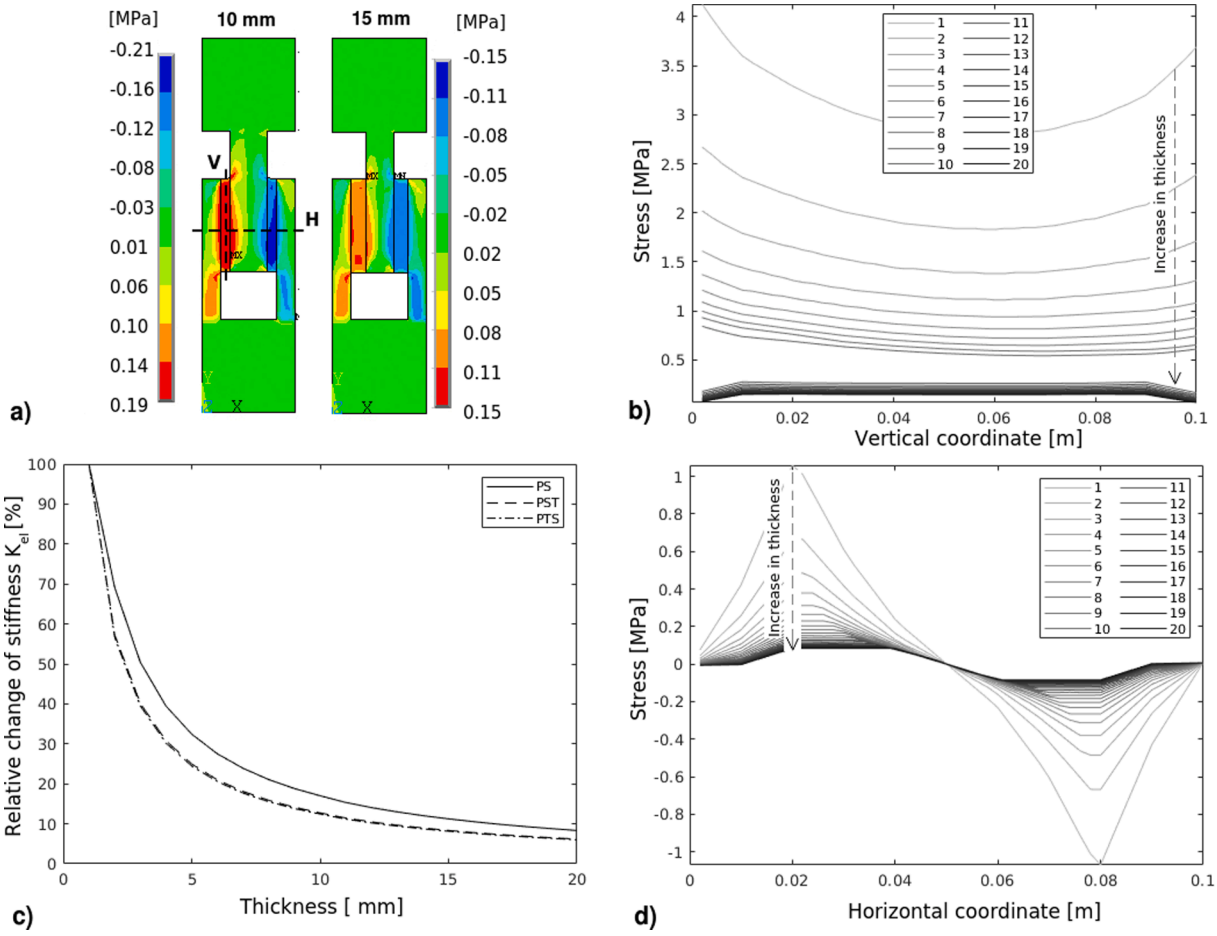

Fig. 9. a) shear stress in XY plane for 10 mm and 15 mm thick adhesive bondline, b) shear stress at vertical path (V) for all simulated thicknesses, c) relative change of k_{el} of the connection with PS adhesive with respect to 1 mm thick bondline, d) shear stress at horizontal path (H) for all simulated thicknesses.

vertical path shows that shear stress is almost constant along the adhesive bond length.

4. Conclusion and future work

An experimental testing program on thick flexible polyurethane adhesive double lap-shear connections was performed with the aim to better understand their performance and explore potential in-use for high performance timber-adhesive composite structures in seismic regions. Mechanical properties used in the design of timber connections, such as stiffness, strength, deformation capacity, ductility, strength degradation, and equivalent damping ratios were derived according to the EN 12512 procedure for three different adhesives and two different bondline thicknesses.

Thicker adhesive bonds provided both higher elasticity and plasticity, which was confirmed by the experiments and by further numerical investigations. This quality may be used to an advantage in timber connection applications that need a relatively strong, but more flexible, adhesive bond. Further, the numerical investigation showed that increasing the thickness of the adhesive substantially reduces maximal shear stress in the adhesive. All three types of tested adhesive connections showed symmetrical cyclic shear behaviour, which is favourable for seismic-resistant shear connections with utilized capacity design approach.

Compared to mechanical dowel-type screwed half-lap connection with a typically used arrangement of fasteners, all tested adhesives displayed significantly higher values in terms of elastic stiffness and strength. Further, adhesive connections also performed better in terms of low cycle fatigue strength degradation compared to mechanical connections. On the other hand, screwed connections performed significantly better in terms of deformation capacity, ductility, and energy dissipation; yet again, adhesive connections were able to elastically deform to substantially higher deformations than screwed connections, meaning they would be able to sustain higher seismic loads with less/no damage. Nevertheless, the tested flexible adhesives can withstand numerous cycles without damage and residual deformation, as it was also shown in [18].

PTS adhesive proved to be the best candidate for further investigation for potential applications due to its relatively good ratio between elastic stiffness and strength capacity compared to other tested adhesives while showing relatively good performance in deformation capacity. With improvements of wood-adhesive bond and increase of the bond length, the connection's deformation capacity and ductility could be further improved. Possible applicability of thick flexible polyurethane adhesive in timber structures might be limited low-to-medium ductile connections or high strength and high stiffness elastically deformable non-dissipative connections in glued-in rod connections, half-lap or step joint connections, secondary elements that are sensitive to brittle failures during seismic events (such as large windows), steel-to-timber flexible connections and potentially even in structural glass-to-timber connections.

Further research on improving bonding capacity by modifying the roughness of wood surface or enhancing the wood-adhesive bonding capacity with different types of primers would be the first next step. In addition, large-scale tests would presumably show the positive influence of increased bonding length and, consequently, also bonding surface, therefore, excluding the negative effect of stress concentration at edges and debonding. Currently, there are no available standard methods for large-scale tests of thick flexible adhesive in timber connections; therefore, further studies are also needed in this aspect. In terms of further numerical investigations, the logical next step would be including fracture phenomenon at the interface between wood and adhesive, as it was investigated for concrete, bonded with thick polyurethane flexible adhesives [21].

Declaration of Competing Interest

The authors declare that they have no known competing financial interests or personal relationships that could have appeared to influence the work reported in this paper.

Acknowledgements

The work has been conducted with the financial support of the European Commission for the InnoRenew project (Grant Agreement #739574) under the Horizon2020 Widespread-2-Teaming program as well as that of the Slovenian Research Agency (Research Core Funding No. [P2-0273] and infrastructural program No. [IO-0035]). Company SIKA is also gratefully acknowledged for providing the material for testing.

References

[1] Ringhofer A, Brandner R, Blaß HJ. Cross laminated timber (CLT): Design approaches for dowel-type fasteners and connections. Eng. Struct. 2018;171:849–61. https://doi.org/10.1016/j.engstruct.2018.05.032.
[2] Izzi M, Casagrande D, Bezzi S, Pasca D, Follesa M, Tomasi R. Seismic behaviour of Cross-Laminated Timber structures: A state-of-the-art review. Eng. Struct. 2018;170:42–52. https://doi.org/10.1016/j.engstruct.2018.05.060.
[3] Gavric I. Seismic behaviour of cross-laminated timber buildings. Italy: University of Trieste; 2013.
[4] Ceccotti A, Sandhaas C, Okabe M, Yasumura M, Minowa C, Kawai N. SOFIE project – 3D shaking table test on a seven-storey full-scale cross-laminated timber building. Earthq. Eng. Struct. Dyn. Earthq. 2013;42(13):2003–21. https://doi.org/10.1002/eqe.v42.1310.1002/eqe.2309.
[5] M.. Valluzzi, E. Garbin, C. Modena, W. Bozza, D. Francescato, Modeling of timber floors strengthened with seismic improvement techniques, Wiad. Konserw. – J. Herit. Conserv. 46 (2016) 69–79. 10.17425/WK46TIMBER.
[6] Larsson G. Proposal of the Shear plate dowel joint. Sweden: Lund University; 2017.
[7] Scotta R, Marchi L, Trutalli D, Pozza L. A dissipative connector for CLT buildings: Concept, design and testing. Materials (Basel). 2016;9:1–17. https://doi.org/10.3390/ma9030139.
[8] Latour M, Rizzano G. Cyclic behavior and modeling of a dissipative connector for cross-laminated timber panel buildings. J. Earthq. Eng. 2015;19(1):137–71. https://doi.org/10.1080/13632469.2014.948645.
[9] Loo WY, Kun C, Quenneville P, Chouw N. Nawawi, Experimental testing of a rocking timber shear wall with slip-friction connectors. Earthq. Eng. Struct. Dyn. Earthq. 2014;43(11):1621–39. https://doi.org/10.1002/eqe.v43.1110.1002/eqe.2413.
[10] Hashemi A, Zarnani P, Masoudnia R, Quenneville P. Seismic resistant rocking coupled walls with innovative Resilient Slip Friction (RSF) joints. J. Constr. Steel Res. 2017;129:215–26. https://doi.org/10.1016/j.jcsr.2016.11.016.
[11] Iqbal A, Pampanin S, Palermo A, Buchanan AH. Performance and design of LVL walls coupled with UFP dissipaters. J. Earthq. Eng. 2015;19(3):383–409. https://doi.org/10.1080/13632469.2014.987406.
[12] A. Baird, T. Smith, A. Palermo, S. Pampanin, Experimental and numerical Study of U-shape Flexural Plate (UFP) dissipators, in: NZSEE Conf., Auckland, New Zealand, 2014: pp. 1–9. http://db.nzsee.org.nz/2014/poster/2_Baird.pdf.
[13] H.J. Blass, M. Schmid, H. Litze, B. Wagner, Nail plate reinforced joints with dowel-type fasteners, in: 6th World Conference on Timber Engineering, Whistler, 2000.
[14] Barile C, Casavola C, Pappalettera G, Vimalathithan PK. Damage propagation analysis in the single lap shear and single lap shear-riveted CFRP joints by acoustic emission and pattern recognition approach. Materials (Basel). 2020;13. https://doi.org/10.3390/ma13183963.
[15] Kwiecień A. Shear bond of composites-to-brick applied with highly deformable, in relation to resin epoxy, interface materials. Mater. Struct. Constr. 2014;47(12):2005–20. https://doi.org/10.1617/s11527-014-0363-y.
[16] Vallée T, Tannert T, Fecht S. Adhesively bonded connections in the context of timber engineering–A Review. J. Adhes. 2017;93(4):257–87. https://doi.org/10.1080/00218464.2015.1071255.
[17] Jeevi G, Nayak SK, Abdul Kader M. Review on adhesive joints and their application in hybrid composite structures. J. Adhes. Sci. Technol. 2019;33(14):1497–520. https://doi.org/10.1080/01694243.2018.1543528.
[18] Rousakis T, Ilki A, Kwiecien A, Viskovic A, Gams M, Triller P, et al. Deformable Polyurethane Joints and Fibre Grids for Resilient Seismic Performance of Reinforced Concrete Frames with Orthoblock Brick Infills. Polymers (Basel). 2020;12:2869. https://doi.org/10.3390/polym12122869.
[19] Sánchez M, Faria P, Ferrara L, Horszczaruk E, Jonkers HM, Kwiecień A, et al. External treatments for the preventive repair of existing constructions: A review. Constr. Build. Mater. 2018;193:435–52. https://doi.org/10.1016/j.conbuildmat.2018.10.173.
[20] Kwiecień A, de Felice G, Oliveira DV, Zając B, Bellini A, De Santis S, et al. Repair of composite-to-masonry bond using flexible matrix. Mater. Struct. Constr. 2016;49(7):2563–80. https://doi.org/10.1617/s11527-015-0668-5.

[21] Zdanowicz Ł, Seręga S, Tekieli M, Kwiecień A. Polymer flexible joint as a repair method of concrete elements: Flexural testing and numerical analysis. Materials (Basel). 2020;13:1–14. https://doi.org/10.3390/ma13245732.
[22] Brunner M, Lehmann M, Kraft S, Fankhauser U, Richter K, Conzett J. A flexible adhesive layer to strengthen glulam beams. J. Adhes. Sci. Technol. 2010;24(8-10): 1665–701. https://doi.org/10.1163/016942410X507759.
[23] K. Rodacki, Z. Bogusław, A. Kwiecień, M. Tekieli, K. Furtak, The Strength of Wooden (Timber)-Glass Beams Combined with the Polyurethane Adhesive - DIC and Finite Element Analysis, in: Struct. Anal. Hist. Constr., RILEM Book, 2019: pp. 323–331. 10.1007/978-3-319-99441-3.
[24] Jelušič P, Kravanja S. Flexural analysis of laminated solid wood beams with different shear connections. Constr. Build. Mater. 2018;174:456–65. https://doi.org/10.1016/j.conbuildmat.2018.04.102.
[25] Angelidi M, Vassilopoulos AP, Keller T. Ductile adhesively-bonded timber joints – Part 1: Experimental investigation. Constr. Build. Mater. 2018;179:692–703. https://doi.org/10.1016/j.conbuildmat.2018.05.214.
[26] K. Śliwa-Wieczorek, B. Zając, T. Kozik, Tests of polymeric adhesive joints in aspect of their application in prefabricated timber structures, Arch. Civ. Eng. 66 (2020) 113–125. 10.24425/ace.2020.131778.
[27] Arkadiusz K, Konrad R, Bogusław Z, Kozik T. In: Mechanical Behavior of Polyurethane Adhesives Applied to Timber Joints in Repair of Historical Timber Structures. Springer, Cham: RILEM Book; 2019. p. 1603–12. https://doi.org/10.1007/978-3-319-99441-3.
[28] S. Zöllig, A. Frangi, S. Franke, M. Muster, Timber structures 3.0 - New technology for multi-axial, slim, high performance timber structures, in: WCTE 2016 - World Conf. Timber Eng., Vienna, Austria, 2016.
[29] Pizzo B, Lavisci P, Misani C, Triboulot P, Macchioni N. Measuring the shear strength ratio of glued joints within the same specimen. Holz Als Roh - Und Werkst. 2003;61(4):273–80. https://doi.org/10.1007/s00107-003-0386-5.
[30] Szeptyński P. Comparison and experimental verification of simplified one-dimensional linear elastic models of multilayer sandwich beams. Compos. Struct. 2020;241:112088. https://doi.org/10.1016/j.compstruct.2020.112088.
[31] SIST EN 302-1:2013 - Adhesives for load-bearing timber structures-Test methods, 2013.
[32] Hasegawa K, Crocombe AD, Coppuck F, Jewel D, Maher S. Characterising bonded joints with a thick and flexible adhesive layer-Part 1: Fracture testing and behaviour. Int. J. Adhes. Adhes. 2015;63:124–31. https://doi.org/10.1016/j.ijadhadh.2015.09.003.
[33] Lasowicz N, Kwiecień A, Jankowski R. Experimental study on the effectiveness of polyurethane flexible adhesive in reduction of structural vibrations. Polymers (Basel). 2020;12:1–21. https://doi.org/10.3390/polym12102364.
[34] M.D. Banea, L.F.M. da Silva, Mechanical Characterization of Flexible Adhesives, J. Adhes. 85 (2009) 261–285. 10.1080/00218460902881808.
[35] Cruz JR, Sena-Cruz J, Rezazadeh M, Seręga S, Pereira E, Kwiecień A, et al. Bond behaviour of NSM CFRP laminate strip systems in concrete using stiff and flexible adhesives. Compos. Struct. 2020;245:112369. https://doi.org/10.1016/j.compstruct.2020.112369.
[36] Cruz JR, Seręga S, Sena-Cruz J, Pereira E, Kwiecień A, Zając B. Flexural behaviour of NSM CFRP laminate strip systems in concrete using stiff and flexible adhesives. Compos. Part B Eng. 2020;195. https://doi.org/10.1016/j.compositesb.2020.108042.
[37] M. Popovski, E. Karacabeyli, Seismic behaviour of cross-laminated timber structures, in: 15th World Conf. Timber Eng. WCTE, Lisbona, 2012.
[38] Gavric I, Fragiacomo M, Popovski M, Ceccotti A. Behaviour of Cross-Laminated Timber Panels under Cyclic Loads. In: Aicher S, Reinhardt H-W, Garrecht H, editors. Mater. Springer, Netherlands, Dordrecht: Joints Timber Struct; 2014. p. 689–702.
[39] Primer Sika ZP. Polyurethane primer for mineral substrate and steel. Data Sheet: Prod; 2014.
[40] ISO 16670 Timber structures — Joints made with mechanical fasteners — Quasi-static reversed-cyclic test method, (2003) 1–9.
[41] EN 12512:2001 Timber structures - Test methods - Cyclic testing of joints made with mechanical fasteners, 2001, 1–18.
[42] Ansys®Academic Research, Release 19.1 (Ansys, Inc., USA), 2019.
[43] Milch J, Brabec M, Sebera V, Tippner J. Verification of the elastic material characteristics of Norway spruce and European beech in the field of shear behaviour by means of digital image correlation (DiC) for finite element analysis (FEA). Holzforschung 2017;71:405–14. https://doi.org/10.1515/hf-2016-0170.
[44] EN 1998-1 (2004) Eurocode 8: Design of structures for earthquake resistance, Part 1: General rules, seismic actions and rules for buildings, (2004).
[45] Gavric Igor, Fragiacomo Massimo, Ceccotti Ario. Cyclic behavior of typical screwed connections for cross-laminated (CLT) structures. Eur. J. Wood Wood Prod. 2015; 73(2):179–91. https://doi.org/10.1007/s00107-014-0877-6.
[46] Ceccotti Ario. New Technologies for Construction of Medium-Rise Buildings in Seismic Regions: The XLAM Case. Struct. Eng. Int. 2008;18(2):156–65. https://doi.org/10.2749/101686608784218680.
[47] Popovski M, Gavric I. Performance of a 2-Story CLT House Subjected to Lateral Loads. J. Struct. Eng. 2016;142:1–12. https://doi.org/10.1061/(asce)st.1943-541x.0001315.